

# A Simple and Controlled Synthesis of Net-like Pd Nanostructure and Their Electrocatalytic Properties toward the Oxidization of Formic Acid

Yun Zhi Fu<sup>1</sup>, Yun Yang<sup>2,\*</sup>

<sup>1</sup> Hainan University College of Materials and Chemical Engineering Institute HaiNan Haikou 570228.

<sup>2</sup> Nanomaterials and Chemistry Key Laboratory, Wenzhou University, Wenzhou, Zhejiang 325027, P. R. China.

\*E-mail: [yzhfu@hainu.edu.cn](mailto:yzhfu@hainu.edu.cn)

Received: 16 November 2011 / Accepted: 30 November 2011 / Published: 1 January 2012

---

Nanostructured Pd networks were synthesized in high yield through the reduction of Pd (acac)<sub>2</sub> using oleylamine as the solvent, reductant and capping agent. The formation of the network Pd nanostructure is due to oriented attachment among the formed primary particles at high temperature. By adjusting the reaction time, concentration of Pd precursor and reaction temperature, their thickness and interconnectivity can be tuned. The prepared nanostructured Pd networks exhibit efficient electrocatalytic activities toward the oxidation of formic acid in acid media. The enhanced electrocatalytic properties of Pd networks can be attributed to the interconnectivity and presence of a large number of active sites on their surfaces.

---

**Keywords:** net-like Pd nanostructure; controlled synthesis; electrocatalytic activities.

## 1. INTRODUCTION

Direct formic acid fuel cells (DFAFC) as a new generation of environment-friendly power sources with high efficiency has attracted much attention [1-3]. Noble Pd or Pd-based materials are frequently-used catalysts for DFAFC [4], which strongly increases its cost and limits its wide applications for increasing price of Pd. Therefore, scientists are trying to develop stagey to reduce the amount of Pd used in catalysts on the premise of keeping catalytic ability. One of method is to improve activity of catalysts. Generally, the Pd atoms on the surface of catalysts which have low-coordination

number act as active site provider, that is, the atoms from surface play a more important role than those inside. Nanoparticles (NPs) has high surface-to-volume atomic ratio which have been demonstrated to be highly active during catalytic reaction, therefore the study about replacing conventional catalysts by using nanoparticles is a very interesting field[4].

It has been reported that morphology of the nanoparticles play critical roles on their activities [5]. Effectively controlling the morphology of nanostructures can provide an opportunity onto improve their catalytic properties and increase their activity planes on mass or specific basis. Inspired by this intention, a variety of colloidal protocols have been used to synthesize shape-adjusted Pd nanostructures, such as wet-chemistry synthesis [6, 7], electrochemical deposition [8, 9], and structural template [10-12]. So far, variously shaped Pd nanoparticles have been fabricated, such as nanopolyhedron [13 14], nanowires [15 16], branched nanostructure [17 18] and nano dendrite [19 20]. Generally, the Pd nanoparticle shape is determined by the enclosed facet and the crystal growth rule always allows the existence of low index facet ( $\{111\}$ ,  $\{110\}$ , and  $\{100\}$ ) [21]. For example, octahedron nanoparticles is bounded by 8  $\{111\}$  and truncated octahedron by 8  $\{111\}$  and 6  $\{100\}$ . The nanoparticles enclosed by above three low index facets have lower activity than other facets. For instance, Sun [13] has reported that 4.5nm Pd NPs could be synthesized via a BTB reduction process in oleylamine media.

The as-prepared Pd NPs gave a surface area of about  $182\text{cm}^2$ , which is higher catalyst activity than the commercial Pd/C nanocatalysts. Wang [18] reported a highly dispersed and uniform palladium nanowire networks synthesized by a controllable, templateless and polyelectrolyte-mediated self-assembly process.

Such nanostructure shows highly active and stable for the formic acid electrooxidation in acid media, demonstrating the promising potential of Pd nanowire networks as effective electrocatalysts for direct formic acid fuel cells. Anshuman [22] reported the fabrication of non-spherical Pd nanostructures prepared using a peptide template. Three different Pd morphologies nanoparticles, short linear nanoribbons, and nanoparticle networks can be fabricated by controlling the Pd: peptide ratio. Capping agent improve catalytic ability.

In this work, we reported a facile, efficient, and controllable route to synthesize Pd network nanomaterials with oleylamine as the solvent, reductant and capping agent. The advantage is (I) no chemical treatment and harsh chemicals are needed as in the case of template method; (II) the shape and size of the Pd nanostructures can be tailored via the pH of the reaction solution and the reducing agents used; (III) the synthesis process is simple and does not require sophisticated equipment and set-ups. The results show that highly dispersed and uniform Pd nanorod networks (NRNs) synthesized by the templateless are highly active than the 4.5nm Pd nanoparticles for the formic acid electrooxidation in acid media for DFAFCs., The prepared nanostructured Pd networks exhibit efficient electrocatalytic activities toward the oxidation of formic acid in acid media and the enhanced electrocatalytic properties of Pd networks can be attributed to the interconnectivity and presence of a large number of active sites on their surfaces. This is very portent for electrocatalytic character in DFAFC in the future.

## 2. EXPERIMENTAL SECTION

### 2.1. Reagents

Oleyl amine,  $\text{LiBH}_4$ , platinum acetylacetonate ( $\text{Pt}(\text{acac})_2$ ) (99.9%, aladdin) ,  $\text{NaBH}_4$  (>96%) and oleylamine ( aladdin ) were purchased from Tokyo chemical industry. All chemicals were used as received without further purification.

### 2.2 The synthesis of Pd nanoparticle

Pd nanorod net-work were prepared as follows: 10 mg  $\text{Pd}(\text{acac})_2$  was dissolved into 5 mL oleylamine ( aladdin ) to form a clear solution with the concentration of 2mg/mL and the mixture was sealed in a stainless steel autoclave with a 40 mL capacity Teflon liner and heated at 180 °C for 12 hrs. After cooling to room temperature, 40 mL ethanol was added to yield a black precipitation which was separated by centrifuging (5000rpm). The obtained precipitations were redispersed in 3 mL chloroform and 10 mL ethanol was introduced to re-precipitate NPs. After centrifuging again, the collected precipitations were dried completely at 45 °C.

### 2.3The characterization of nanoparticles

For TEM, HRTEM and EDX, corresponding purified colloids are deposited on copper grids coated by carbon membrane and dried at 80 °C. After the water is removed completely, the sample is observed on 300 KV Tecnai G2 F30 S-Twin microscopes with an attached EDX. The Pd nanostructure was analyzed by transmission electron microscopy (TEM) using JEOL JEM 2000EXmicroscope at an accelerating voltage of 200 kV. High resolution transmission electron microscopy (HRTEM) images were obtained using a FEI TecnaiF20 microscope operated at 200 kV. TEM specimens were prepared by drop-casting a suspension of platinum nanocrystals in chloroform onto carbon-coated copper grids. The electrochemical performance of the electrodes was investigated by using a PARSTAT 30 Advanced Electrochemical System.

### 2.4The preparation of Pd NRN/C electrocatalysts

A method developed by Sun was employed to prepare Pd NPs/C catalysts [29]. In a typical preparation, above synthesized Pd NPs (10mg) were dissolved in hexane and mixed with an equal amount of carbon black (Vulcan XC-72). Resulting mixture was sonicated for 2 h. Acetic acid was then added and the mixture was stirred at 70 °C for 12 h. The black carbon with Pd NPs was precipitated out by centrifugation at 5000 rpm and washed with ethanol three times. The Pd/C NPs

were recovered by adding acetone and weighed after acetone was evaporated. A measured amount of de-ionized water was added, resulting in a 1 mg/mL solution. This mixture was sonicated for 1 h to ensure uniform distribution. All catalytic studies were carried out using 20  $\mu$ L of this catalyst.

### 2.5 Electrochemical Measurements

Electrochemical measurements were carried out in the electrolyte consisting of 0.5 M H<sub>2</sub>SO<sub>4</sub> and 0.5 M formic acid by using conventional three-electrode cells with a Pt flake of 1 cm<sup>2</sup> area as the counter electrode, an Ag/AgCl-KCl (saturated) electrode as the reference electrode, and a glassy carbon (GC,  $\Phi=3$ mm) loaded with active nanocatalysts as the working electrode. All potentials were referenced to Ag/AgCl-KCl (saturated). Before each experiment, the GC electrode was polished with the slurry of alumina nanoparticles to a mirror. A 20  $\mu$ L aliquot suspension of the catalyst was drop-cast onto the GC electrode and dried under vacuum. The catalyst was fixed on the electrode by depositing a layer of 0.1% nafion solution. The amount of metals in a catalyst was quantified by TGA. The electrochemical performance of the electrodes was investigated by using a PARSTAT 30 Advanced Electrochemical System. The cyclic voltammograms (CV) of methanol oxidation were measured at the scan rate of 20 mV/s in the potential range of 0 V to 1.0 V at room temperature. The chronoamperometry curves were obtained by polarizing the electrode at 0.65 V for 2000 s in the above-mentioned electrolyte. Before each test, the solution was purged with N<sub>2</sub> for 5 min to eliminate the dissolved oxygen.

## 3. RESULTS AND DISCUSSION

### 3.1 TEM, HR-TEM and EDAX characterization

The Pd nanoparticles capped by oleyl amine can be dispersed in nonpolar solvent easily. After the Pd colloid is dried on copper grid with carbon membrane, they were observed with TEM and results are shown in Fig. 1 a. Figure 1a shows the TEM image of the prepared Pd nanorod networks sample, obtained at a Pd concentration in OAm of 2mg/ML after a reaction time of 12 hours. A number of bending nanorods interconnected to form a net-like nanostructure could be clearly observed. The average circular diameter of the networks Pd nanostructure obtained by measuring the width of the nanorod was about 4 nm. The number density of the rods can be tuned by adjusting the concentration of Pd precursors, where high concentration yield more thick networks. The Pd networks nanostructure further analyzed by using HR-TEM as shown in figure 1b. It can be seen the prepared particles have samples shows a good crystalline structure with well-defined lattice fringes. The d spacing for adjacent lattice fringes measured from several different points was 2.30  $\text{\AA}$ , which corresponds to the mean value of the (111) planes of face-centered cubic (fcc) of Pd, indicating that most of the exposed facets of the Pd nanorod networks were {111}. Also, the sample was deposited on the copper grid for EDAX

analysis, which demonstrated that the net-like nanostructure was composed of pure Pd without any other species.

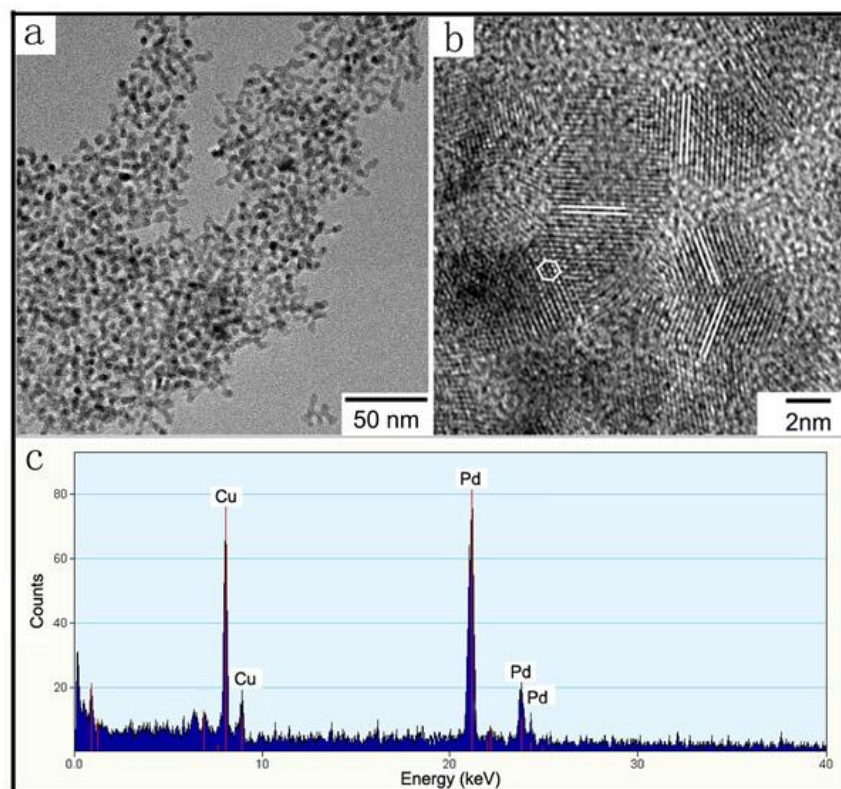


**Figure 1.** TEM images of the synthesized net-like Pd nanostructures (a) and the HRTEM images (b). EDAX of the Pd nanorod network (c)

### 3.2 time-dependent shape evolution of Pd(acac)<sub>2</sub>

To investigate the evolution process of the Pd nanostructure, samples with various reaction times were conducted by TEM and HR-TEM analysis. Fig. 2 shows the synthesized Pd nanostructure, which are highly dispersed along the TEM grid surface. Characterization of the samples by TEM demonstrated a shift in particle morphology. The sample with a reaction time 2h (Fig 2a) was demonstrated the formation of irregular spherical Pd nanoparticles; however, when the reaction time increased to 4h (Fig 2b), the formation of V-like short nanorod was observed. This elongation effect was further evident when the reaction time was increased to 8h (Fig 2c) and 12h (Fig 2d) respectively where branched Pd NRNs are observed in the sample. Note that for reaction time excess 12h, no change was observed. From the observed structural changes, this suggests that a specific growth mechanism controls the morphology of the final structure such that long reaction time results in the formation of the interconnected branched structures.

Further, high-resolution TEM analysis of the materials was conducted to fully characterize the structures. HR-TEM analysis of the Pd nanoparticles prepared from the sample is presented in (fig 2 e-h). Hexagonal close packing of the Pd atoms is observed in the HR-TEM image of the materials and is denoted in the figure.

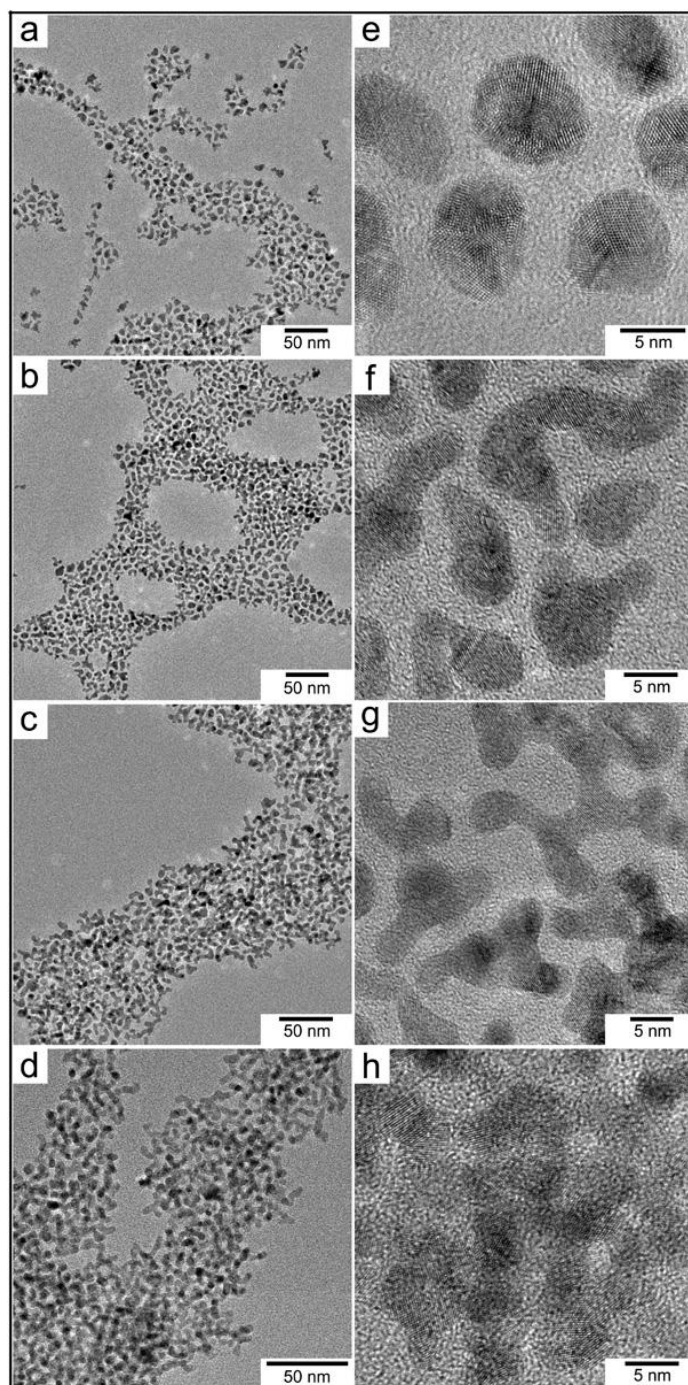


**Figure 2.** TEM images of the Pd nanostructure with different reaction time: (a-d) 2h, 4h, 8h and 12h; (e)-(h) is the corresponding HR-TEM images.

Fringes of the Pd (111) lattice are observed with a d-spacing of 2.3 Å slight time prolong to 4h indicated that V-type nanostructure and irregular short rods were prepared under such condition as shown in Fig. 2f. There is a little distinction in shape to the sample with 2h reaction time. Clear lattice fringes are observed from these nanoparticles with a d-spacing of 0.23nm, which fits with the d-spacing of the (111) plane of fcc Pd. Fig. 2g shows the HRTEM images of the samples with reaction time 8h. Analysis of the material shows that the bifurcated Pd nanostructure is in stark contrast to the irregular spherical nanoparticles fabricated less than 2h reaction time. Characterization of the sample with 12h presented in Fig. 3h demonstrated the formation of the Pd net-work is more inter-connected. HR-TEM analysis of the sample shows that the materials are polycrystalline in nature with Pd (111) lattice fringes of 0.23nm, which has been observed for all samples studied in the present analysis.

### 3.3 The time-dependent shape evolution mechanism of net-like Pd nanostructure

This time-dependent shape evolution also provides experimental evidence on how the Pd nanorod network formed from the seed crystals. Fig 3 shows the representative HR-TEM images of the sample with different reaction time.

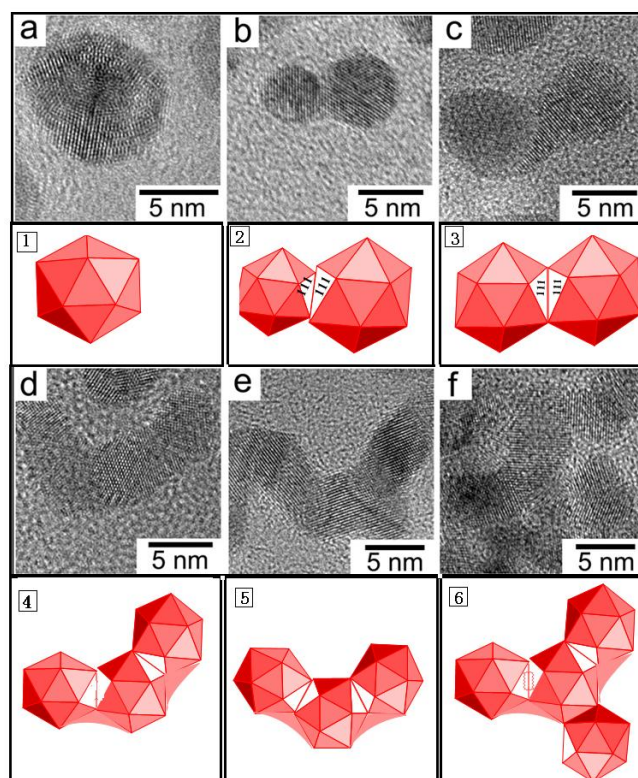


**Figure 3.** HR-TEM images showing the grow stages: (a) single particle; (b) and (c) two particles connected through MA or TA growth; (d) and (e) three particles connected through MA or TA growth; (f) the final network nanostructure. 1, 2, 3, 4, 5, 6 showing as (a), (b), (c), (d), (e), (f) skeleton map of the grow stages of Pd nanoparticles

From the evolution of the structure observed, it seems that the primary particles grow into together through attachment and the attachment mostly occurred on (111) facets. Such net-like structure are formed through twinning attachment or match attachment [24], but not a physical aggravation.

The attachment is mostly driven by the interplay between the binding energy of capping agents on NPs surfaces and the diffusion of atoms at the interface upon the collision of primary nanoparticles[24].

A possible synthetic mechanism could be described as follows: initially, a larger number of nucleation sites develop within oleylamine system during thermal reduction of long chain amine and the precursors react to form seeds and subsequently grow into nanoparticles until the precursors exhausted.

These nanoparticles are composed of (111) facets and stabilized by capping agents and the adsorption of the oleylamine molecular on the Pd surface is a dynamic equilibrium process. Owing to the weak binding between capping agent and (111) facets of Pd at high temperature, the nanocrystal surface is loosely protected and the vander Waals interaction is strong enough to overcome the capping effect [22], the surface atoms can then be in direct contact with each other upon the collision between two particles, and diffuse across the interface to form anisotropic structures.

The key factors in determining the formation of nanorods from primary nanoparticles should largely be governed by both the spontaneous exposure of nanocrystal surfaces and the likelihood of bond formation at the interface.

### 3.4 The effect from the amount of $Pd(acac)_2$

The effect of the precursor concentration was investigated to examine its role in shape control. Figure 4 shows the TEM images of the products at a precursor's concentration of 0.0025 mmol/mL and 0.025 mmol/ mL, respectively. In these experiments, the reaction time kept for 12 hours for both of the samples.

Noticeably, with low concentration, nanorod network could no longer be observed, Figure 4a and b. Unlike the above cases, the heterogeneous nanostructure did not attach together to form a net-like structure, most likely due to the particles are sufficiently spaced within the solution such that the interparticle distance is maximized to prevent interactions between individual nanoparticles that would lead to their attachment.

With the concentration increased, the networks were observed, but with higher density and lower aspect ratio of the nanorods. This observation can be explained by the large number of nucleation sites and limit space for the nanoparticles. Due to this effect, the distance between nanoparticles decreased and easily aggregated to form a more complex and disorderd network. By 12 h, ripening process caused the smoothening of the nanocrystals while the overall shape and dimension were maintained.

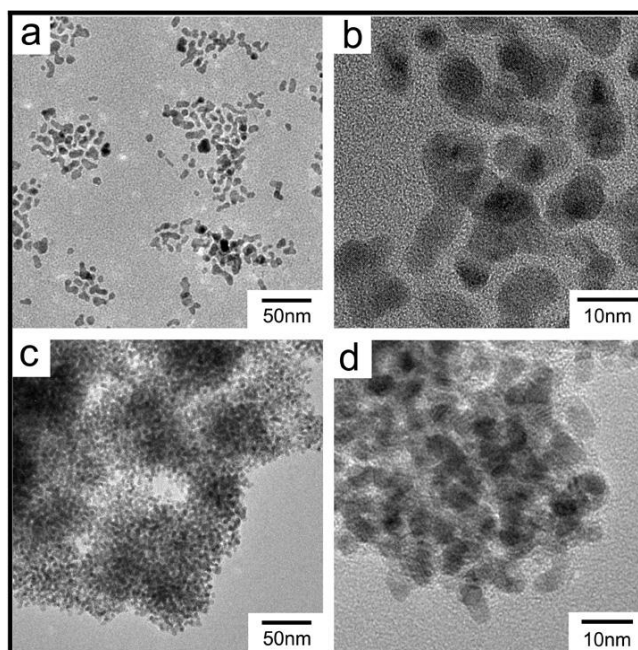


**Figure 4.** TEM images of Pd samples obtained at a Pd concentration of 0.0025 mmol/mL (a) and 0.025 mmol/ mL (b)

### 3.5 The effect of the temperature

The effect of the temperature on the formation of Pd nanorod network was investigated. Figure 5 shows the TEM images of the Pd nanorod network at 200 °C. The samples were net-like structure just like a polyporous sphere. It was difficult to analyze the nanocrystals and the diameter because of their aggregation and overlap. At 200 °C, Pd(acac)<sub>2</sub> could be reduced by long chain amine. And the temperature was close to decomposition of Pd (acac)<sub>2</sub>, thus, the shape control via a kinetically controlled process became little by little, particularly after a relatively long reaction time period that the ripening process smoothed out the surfaces of the Pd nanostructure and the long rods seldom observed [23]. In fact, such reaction system turned into thermodynamically stable by 12 hours.

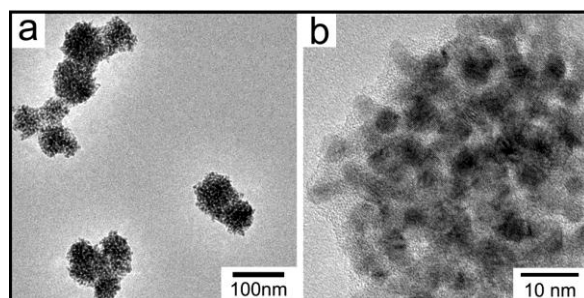


**Figure 5.** TEM images of samples obtained at a concentration of 0.005mmol/ml after a reaction time of 12h at 200 °C

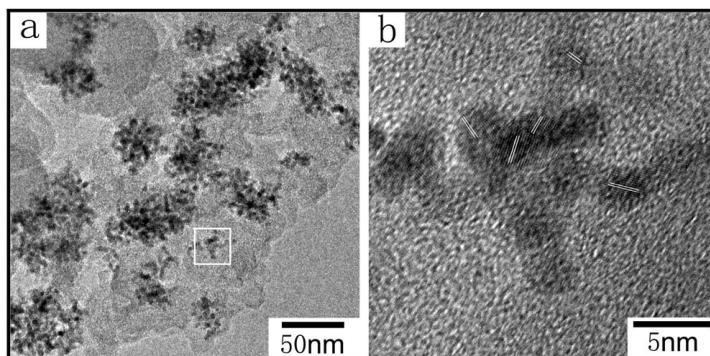


**Figure 6.** (a) TEM image of the prepared Pd NRN/C catalyst (b) corresponding HR-TEM image of the square region in (a).

### 3.6 The catalytic properties in oxidization of formic acid

The electrocatalytic activity of Pd nanorod networks for the electrooxidation of formic acid in acid medium was studied at room temperature. Figure 6 shows the TEM micrograph of the Pd NRN/C electrocatalysts prepared by sonic the Pd NRNs and high surface area carbon (XC-72). It can be seen that the high dispersity of the Pd NRNs on the carbon and retain the net-like structure well. The crystalline remain well not destroyed during the sonic process. Lattice distance of 2.3 still shows that the facet exposed on the carbon finally is (111).

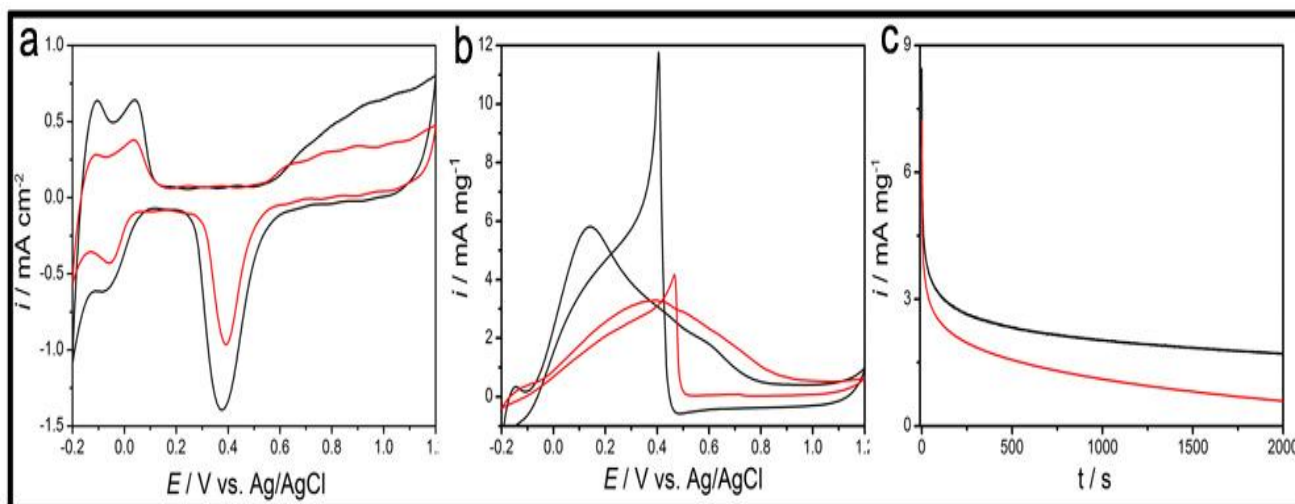


**Figure 7.** (a) Cyclic voltammograms of Pd NRT and 4.5nm Pd NPs modified GC electrode in a  $N_2$  sparged  $H_2SO_4$  (0.5M) solution at scan rate of  $50 \text{ mVs}^{-1}$ . (b) Cyclic voltammograms of formic acid oxidation at the Pd NRT and Pd NPs modified GC electrode, in  $H_2SO_4$  (0.5M) solution containing formic acid (0.5M). Scan rate:  $50 \text{ mVs}^{-1}$ . (c) chronoamperometric curves for formic acid electrooxidation at 0.1 V versus Ag/AgCl on Pd NWN/C and Pd NP/C electrodes in a 0.5 M  $H_2SO_4$  + 0.5 M HCOOH solution.

The Pd nanorods networks and the Pd NPs were tested as nanoelectrocatalysts for comparison to study their catalytic activity. Figure 7 shows the cyclic voltammograms (CVs) of GC electrodes modified with the Pd nanorod network and Pd NPs obtained in 0.5 M  $\text{H}_2\text{SO}_4$  at a scan rate of 50 mV/s. In both cases, Pd loadings were adjusted to 0.01 mg. As shown in figure 7a, typical hydrogen adsorption/ desorption [25] were observed. The electrochemically active surface areas (ECSA), which were calculated by measuring the Coulombic charge for oxygen desorption [26]. It is found that the ECSA value of Pd nanowire network (85.7  $\text{m}^2/\text{g}$ ) is significantly higher than that of the Pd NPs catalyst (52.4  $\text{m}^2/\text{g}$ ). Figure 7b shows the CVs of formic acid oxidation at Pd nanowire network and Pd NPs modified GC electrode in a 0.5 M  $\text{H}_2\text{SO}_4$  solution containing 0.5 M formic acid. The current densities are normalized with respect to the mass. Typical well separated anodic peaks in the forward and reverse scan associated with formic acid oxidation were observed.

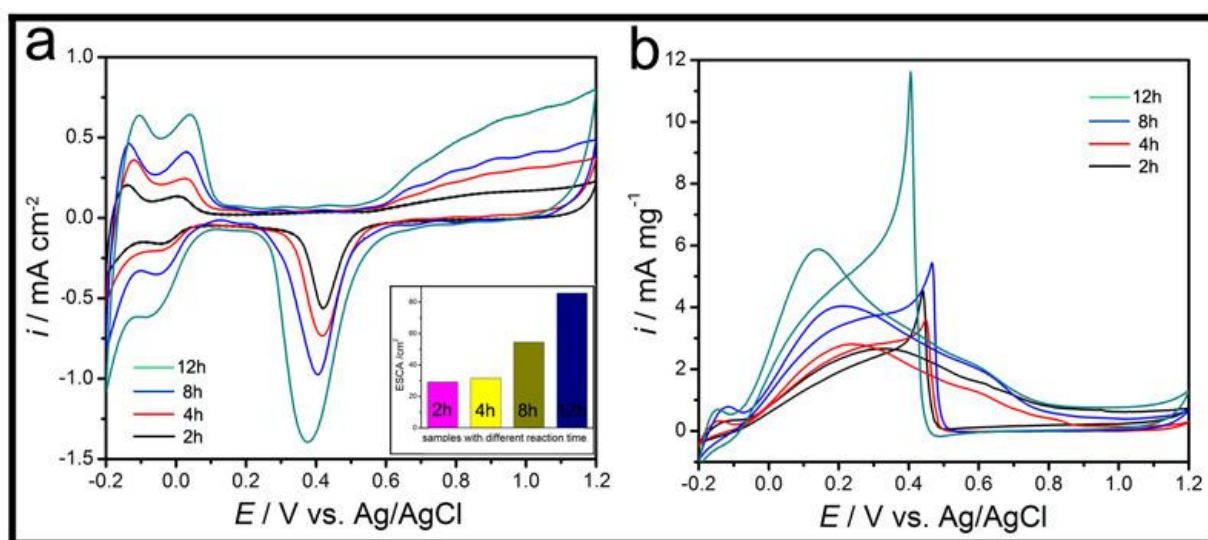


**Figure 8.** (a) Cyclic voltammograms of net-like Pd nanostructure (a), bending rods crossing (b), shot rods (c) modified GC electrode in a  $\text{N}_2$  sparged  $\text{H}_2\text{SO}_4$  (0.5 M) solution at scan rate of 50 mV/s. (b) Cyclic voltammograms of formic acid oxidation at the net-like Pd nanostructure (a), bending rods crossing (b), shot rods (c) modified GC electrode, in  $\text{H}_2\text{SO}_4$  (0.5 M) solution containing formic acid (0.5 M). Scan rate: 50 mV/s. (c) histogram of ECSA

The first oxidation peak observed on Pd net-like at 0.14V [27] assigned to the oxidation of  $\text{HCOOH}$  is lower than that of the Pd NPs. The mass current density for  $\text{HCOOH}$  oxidation in Pd nanorods network (solid line) was found to be 5.89, about 2 times higher than those of the Pd NPs catalysts. The electrochemical stabilities of the Pd nanorods network and Pd NPs for formic acid electrooxidation were also investigated by chronoamperometric experiments at 0.1 V versus Ag/AgCl (Figure 7c). The polarization current for the formic acid oxidation shows a rapid decay, similar to that on the Pt-based electrocatalysts[28]. The decay in the anodic current could be related to the

intermediate species poisoning of the HCOOH electrooxidation via the CO pathway or to the deactivation of the Pd electrocatalysts by an organic poisoning species [29, 30]. But it is noticeable that the current decays associated with the poisoning of the intermediate species on the Pd nanorods network are much slower than that on the Pd NPs, indicating the high tolerance in comparison with the conventional Pd NPs. This indicates that a Pd NRN structure enhances the electrochemical stability of Pd electrocatalysts for the formic acid oxidation in acid solution. All of the above data reveal that Pd nanorods network exhibit higher catalytic activity and faster kinetic for formic acid oxidation than conventional Pd NPs, most likely due to the high density of active sites and large surface area of nanorods nanostructures with high aspect ratio. This result indicated that this structure are electrochemically more accessible, which is very important for the electrocatalytic reactions.

Figure 8 shows the electrocatalytic activities of Pd NRNs synthesized with the different reaction time. The CVs obtained in 0.5 M H<sub>2</sub>SO<sub>4</sub> at a scan rate of 50 mV/s was used to study their surface properties, as shown in a.

It is found that the sample with reaction time of 12h have the highest ESCA value, is up to 85.7 m<sup>2</sup>/g and the sample with reaction time of 2h have the lowest 29.2m<sup>2</sup>/g. With the decrease of the reaction time, the ESCA value decreases significantly, as shown in b. The electrocatalytic properties of formic acid oxidation on samples were tested in a solution containing 0.5 M H<sub>2</sub>SO<sub>4</sub> and 0.5 M formic acid and the result was shown in c. Obviously, with the increase of the reaction time, the increased mass current density from the minim value of 2.5 to 5.89, and the gradual shift of HCOOH oxidation peak from 0.35V to 0.14V suggest that the samples with 12h reaction time shows good dispersivity and well-interconnected network structure. The present results indicate that interconnectivity of Pd NRNs is an important factor for the high electrocatalytic activity for the electrooxidation of formic acid probably due to the effective electronic conduction and passage through the highly interconnected nanorod networks for the electrochemical oxidation reactions.

So, it is worthwhile to say that higher activity in electrochemical performance observed can probably be attributed to two major factors: (1) The well-dispersed and high aspect ratio of the nanowire network result in a higher ECSA than conventional Pd NPs; (2) the interconnectivity of the networks provides a number of active sites and the highly interconnected nanostructure are effective for electronic conduction.

#### 4. CONCLUSIONS

In summary, we present a simple method of Pd nanorods network using Pd(acac)<sub>2</sub> and oleylamine. Different Pd nanostructure can be obtained just adjusting the reaction time. Pd NRNs with a high aspect ratio, uniform dispersion and high interconnectivity were obtained at 180°C for 12 hours. Most important, the Pd NRN/C electrocatalysts show a much better electrocatalytic activity and better stability than conventional Pd NP/C electrocatalysts. The results indicate that Pd NRNs are promising

high performance electrocatalysts in DFAFCs. The templateless method for the synthesis of the nanorod network structure is also advantageous as compared to other methods such as the template-based method, being simple and avoiding the use of hard templates and environmentally unfriendly chemicals, demonstrating a new and powerful approach for the development of high-performance electrocatalysts for fuel cells.

#### ACKNOWLEDGMENT

This work was supported by the from, Hainan province natural science foundation of china (Grant Number (11009), PH.D science and technology project Hainan university (kyqd1050), NSFC (21101120), Zhejiang science and technology project (2010C31039), Zhejiang natural science program (Y4110391), Lucheng science and technology project (T100106).

#### References

1. C. Ricea, S. Haa, R.I. Masela, and A. Wieckowskib, *Journal of Power Sources*, 115 (2003) 229.
2. H.X. Zhang, C. Wang, J.Y.Wang, J. J. Zhai, and W. B. Cai, *J. Phys. Chem. C*, 114 (2010) 6446.
3. P. Waszczuk, T. M. Barnard, C. Rice, R.I. Masela, and A. Wieckowski, *Electrochemistry Communications*, 4 (2002) 599.
4. B. J.Wang, *Power Sources*, 152(2005) 1.
5. R. Narayanan , A. Mostafa, and E.Sayed, *Nano Letters*,4 (2004)1343.
6. Y Xiong, H Cai, B. J. Wiley, J .Wang, M. J. Kim, Y. Xia , *J. Am. Chem. Soc.*, (1292007) 3665.
7. Y. Xiong, J .M. McLellan, Y. Yin, and Y. Xia, *Angew. Chem. Int. Ed*,46 (2007)790.
8. Y. W. Chung, I .C. Leu, J .H. Lee, J. H. Yen, M. H. Hon *J. Electrochem. Soc.*, 154 (2007) 77.
9. D. C. Yang, G. W. Meng, S. Y. Zhang, Y. F. Hao, X. H. An, Q. Wei, M. Ye, and L. D. Zhang *Chem. Commun.*(2007) 1733.
10. M. S. Sander, A. L .Prieto, R. Gronsky, T. Sands and A .M .Stacy, *Adv. Mater*, 14(2002 )665.
11. W.C. Yoo and J. K. Lee, *Adv. Mater*, 16 (2004)1097.
12. Y.Zhang, G.H.Li, Y.C.Wu, B.Zhang, W.H.Song and L.Zhang *Adv. Mater*, 14(2002)1227.
13. a.V.Mazumder and S.H.Sun *J. Am. Chem. Soc.*, 131(2009)4588.b.Z.Q.Yang, and K. J. Klabunde, *Journal of Organometallic Chemistry*, 694 (2009) 1016.
14. Qingsheng Liu, J Chris Bauer, Raymond E Schaak, and Jack H Lunsford 2008 *Angew. Chem. Int. Ed.* 47, 6221 –6224
15. Q.M.Shen, Q.H.Min, J.J.Shi, L.P.Jiang, J.R. Zhang, W.H. Hou and J.J. Zhu *J. Phys. Chem. C*, 113 (4) (2009)1267.
16. B.K.Lim, J.G.Wang, P H. C. Camargo, C.M. Copley, M.J. Kim, and Y.N.Xia, *Angew. Chem. Int. Ed*, 48(2009) 1.
17. R. E. Schaak, A. K. Sra, B. M. Leonard, R. E. Cable, J. C. Bauer, Y. F. Han, J. Means, W. Teizer, Y. Vasquez, and E. S. Funck, *J. Am. Chem. Soc.*, 127(2005) 3506.
18. S.Y.Wang, X.Wang and S. P. Jiang *Nanotechnology*, 19 (2008) 455602.
19. J.Watt, S. Cheong, M. F. Toney, B.Ingham, J.Cookson, P. T. Bishop and R. D. Tilley, *ACS Nano*, 4 (1) (2010) 396.
20. J. Watt, N. Young, S. Haigh, A. Kirkland, and Ri. D. Tilley *Adv. Mater.*21 (2009) 288.
21. Y. W. Lee, M.J. Kim, Y. Kim, S. W. Kang, J. H. Lee and S. W. Han *J. Phys. Chem. C*,114 (17)(2010) 7689.

22. A.Jakhmola, R. Bhandari, D. B. Pacardo and M. R. Knecht *J. Mater. Chem*,20 (2010)1522.
23. S. Maksimuk, X.W. Teng and H. Yang *J. Phys. Chem. C* 111 (39)(2007) 14312.
24. Z.M. Peng, H.J.You and H.Yang *ACS Nano*, 4 (3)(2010) 1501.
25. Gomez R, Orts J M, Alvarez-Ruiz B L, Feliu J 2004 *J. Phys. Chem. B*, 108, 228.
26. R. I.Woods, *Electroanalytical Chemistry: A Series of Advances* Bard, A. J., Ed.; Marcel Dekker: New York, 1974; Vol. 9, 1-162.
27. H.Meng, S.H Sun, J.P. Masse and J.P.Dodelet *Chem. Mater.* 20 (22) 2008 6999.
28. S.Y.Uhm, S.T.Chung and J.Y.Lee *Electrochem. Commun.* 9(2007)2027.
29. W.S.Jung, J.H.Han and S.Ha *J. Power Sources*, 173(2007)53.
30. Y.M.Zhu, Z.Khan and R.I.Masel *J. Power Sources*, 139 (2005) 15.